COMPARATIVE SYSTEM DYNAMIC MODELING OF A CONVENTIONAL AND HYBRID ELECTRIC POWERTRAIN

M. Awadallah, P. Tawadros, P.Walker, and N. Zhang
FEIT, University of Technology Sydney

ABSTRACT: Hybrid Electric Vehicles (HEVs) provide many known benefits over conventional vehicles, including reduced emissions, increased fuel economy, and performance. The high cost of HEVs has somewhat limited their widespread adoption, especially in developing countries. Conversely, it is these countries that would benefit most from the environmental benefits of HEV technology. As part of our ongoing project to develop a cost-effective and viable mild HEV for these markets, dynamic simulations are required to ensure that the proposed designs are to achieve their desired targets. In this paper, mathematical models of the powertrain are used to analyze and compare the dynamics of both a conventional power train and one with the addition of components required for the Mild Hybrid system. Using Matlab and Simulink, simulations of both powertrains under particular driving conditions are performed to observe the advantages of the MHEV over conventional drivetrains. These benefits include torque-hole filling between gear changes, increased fuel efficiency and performance.

1 INTRODUCTION

Driving comfort, shifting quality and improved driveability with low manufacturing costs have become strongly aligned with mild hybrid electric powertrains, which allow for a good opportunity for improvement (Kuo, 2011). We discuss a low-power electric motor mounted on the transmission output shaft coupled to a controlled power source, allowing for increased functionality of the powertrain along with a reduction in the torque hole during gear changes. This configuration allows for improved driving performance (Sun and Hebbale, 2005). Primary input signals to the motor controller are; clutch position, ICE load (calculated from speed and throttle angle), and selected gear. The electric machine's function is to eliminate or reduce the torque hole during gear changes by providing a tractive force when the clutch is disengaged. In addition to this, it can provide damping for torque oscillation, particularly during gear changes and take-off (anti-jerk). The electric motor may also act as a generator under certain driving situations (Wagner, 2001).

This paper seeks to research the dynamics of a front wheel drive mild hybrid electric powertrain. A detailed analysis of the system with numerous degrees of freedom is suggested. The resulting equations of motion are written in an indexed form, making it easily implemented into a vehicle model. Lumped stiffness-inertia torsional models of the powertrain will be developed for different powertrain states for the purpose of investigating transient vibration. The major powertrain components (engine, flywheel, transmission, and differential) are lumped as inertia elements which are interconnected with torsional stiffness and damping elements to represent a multi-degree of freedom model of the powertrain (Crowther and Zhang, 2005, Crowther et al., 2007). By modeling the powertrain, possible improvements can be identified when using the electric drive unit. A comparison between the mild hybrid powertrain with a traditional manual transmission driveline is made, with a focused analysis on the lower gears. This is done because in the lower gears the torque transferred to the drive shaft is greater, along with the deflection in the shaft. This means the shaft torsion is higher at lower gear ratios, resulting in larger oscillations. This paper will conclude with the role of integrated powertrain control of both the engine and motor in minimizing torque-hole. High-quality shift control is critical to the reduction of torque-hole and vibration of the powertrain.

1.1 *SHIFT PROCESS ANALYSIS*

For the MT shift quality control, the shift process analysis proves essential. This involves the disengagement and engagement of a single clutch connecting the transmission to the power source. Three

phases encompass the shift process. The first phase involves the disengagement of the clutch and is characterized by a rapid reduction in torque transmission to zero. The second phase, also known as the gear selection phase, is characterized by a fully disengaged clutch and torque-hole, as well as minor torque oscillation from the synchronization of the selected gear. The final phase is the inertia phase, characterized by a large torque oscillation as the clutch slips during re-engagement. At the attainment of a constant speed ratio, the speed of the powertrain is equal to the speed of the vehicle, and the clutch is fully engaged (Galvagno et al., 2009). Factors that influence the shift process include the magnitude of transmitted torque before and after the gear change and the speed of clutch disengagement and engagement. Figure 1 represents an example of measured vehicle data for half-shaft torque (with torque fill during shifts) (Baraszu and Cikanek, 2003).

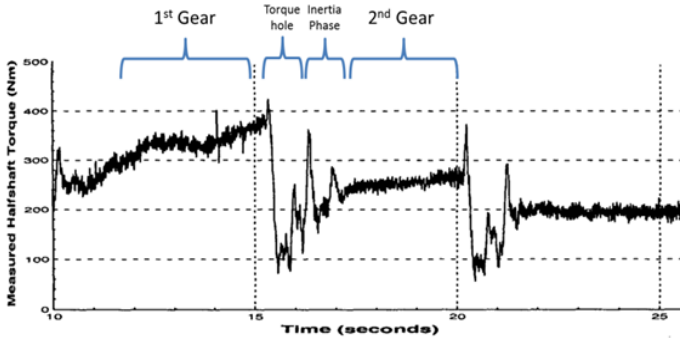

Figure 1. Actual Half-shaft torque with Fill-in.

2 POWERTRAIN MODELLING

The model developed uses a simple empirical engine element utilizing a three-dimensional lookup table. This element is inserted into two powertrain models which are both presented. This section shows the mathematical models of each configuration using eight degrees of freedom for the mild HEV powertrain, compared to seven degrees of freedom for a conventional powertrain.

2.1 *Powertrain equipped with motor*

Figure 2 is representative of a basic mild hybrid transmission powertrain. The powertrain requires a single dry-plate clutch interfacing between the engine and transmission. In a conventional manual transmission, the clutch must be released before synchronization to isolate the synchronizer from engine inertia. Figure 2 also shows the remainder of the powertrain. This includes the electric propulsion system (EPS) which is permanently coupled to the transmission output shaft. The EPS can directly drive the wheels in this configuration, which provides a post-transmission parallel type hybrid vehicle powertrain. As the motor is downstream of the transmission, it ultimately has a fixed constant speed ratio to the wheels via the final drive. As the intended profile for use involves short pulses of high power for torque-filling, the peak mechanical power figure is just as significant as the continuous output to consider. Brushless motor drive is widely used for EV and HEV applications (Zeraoulia et al., 2006, Sharma and Kumar, 2013, Chang, 1994). A 10 kW electric machine satisfied most requirements for torque fill in during gear change. It also provided sufficient power for use in improving vehicle efficiencies under high demand or low engine efficiency conditions (Wagner and Wagner, 2005). The noticeable limitation of this vehicle configuration is that there was no potential to isolate the EM from the wheels, resulting in incidental losses while the motor was freewheeling. Standard synchronizers that are popular in manual transmissions were used to achieve speed synchronization during gear shifting. These synchronizers have low cost and high reliability. Material savings may be found by removal of the synchronizers and replaced by usage of electronic throttle control to accomplish speed synchronization, due to the nature of the mild HEV system proposed. In saying this, these savings presume that speed synchronization may be accomplished with a very high degree of accuracy. The inclusion of synchronizers, however, means that the accuracy of the speed synchronization may be reduced thus improving system response. In addition to this, the savings do not necessarily eventuate into reduced cost due to the current economies of scale. For these reasons, this option is not followed through. The powertrain is essentially a basic post-transmission parallel hybrid configuration. It uses a low-powered four-cylinder engine coupled to a five-speed manual transmission through a robotically actuated clutch. A motor is connected to the transmission output shaft, before the final drive. The literature includes some similar architectures to that proposed (Baraszu and Cikanek, 2002, Rahman et al., 2000, Aoki et al., 2000). Of these, Baraszu (Baraszu and Cikanek, 2002) most closely resembles the architecture that is suggested. However, the architecture outlined in this paper is simpler by the omission of the motor clutch.

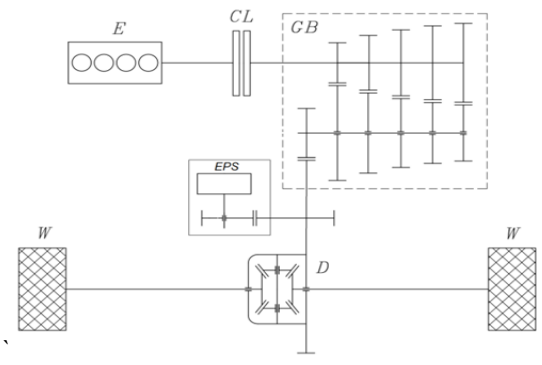

Figure 2. Generalized powertrain layout with hybridization.

It is necessary to extend the research to consider the vibration of the powertrain as well as control of clutch and motor, in order to ensure a complete study of system response. The powertrain model is divided into the following subsections; the engine model, motor model, powertrain inertia model, and vehicle resistance torques model. These models are discussed below.

2.2 *Powertrain lumped model formulation*

The powertrain is modeled using torsional lumped parameters to capture the shift characteristics of the system. Inertia elements represent the major components of the powertrain, such as engine, flywheel, clutch drum, clutch plate, synchronizer with final drive gears, shafts, differential, electric motor, wheels and vehicle inertia. These are exposed to various loads, including rolling resistance and air drag. Torsional shaft stiffness is represented by spring elements connecting major components and losses are represented as damping elements. Figure 3 shows the model layout of a motor mounted on a front wheel vehicle. The application of assumptions can help to minimize the complexity of the powertrain. The first step is to lump inertia of idling gears in the transmission, and primary gear and synchronizer inertias. By doing this, it removes erroneous transmission components. An assumption is made that there is no backlash in the gears or engaged synchronizers, eliminating high stiffness elements in the model. Further based on this assumption, there is a reduction in computational demand. Finally, symmetry in the wheels and axle eventuates in the ability to group these inertias together as a single element. Further losses in transmission and differential are modeled with grounded damping elements.

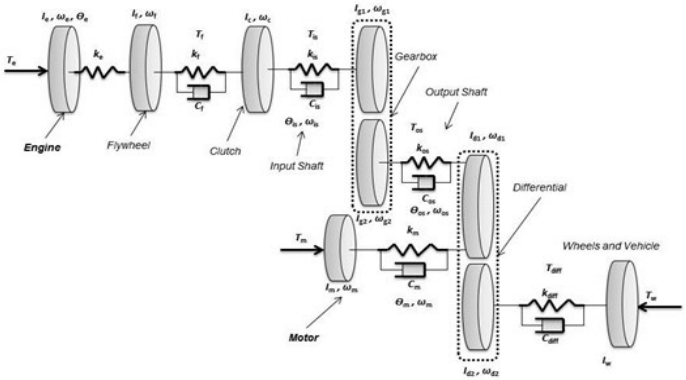

Figure 3. Lumped parameter model for a mild HEV equipped powertrain.

Using the procedures defined by Rao (Rao, 2011) for torsional multi-body systems in equation (1), the lumped parameter model is then constructed. Free vibration and forced vibration analysis can be conducted using the equation of motion. Idling gears are lumped as additional inertia on gears targeted for shifting. Backlash in gears is overlooked as frequencies excited in lash are generally significantly higher than the main powertrain natural frequencies of 3 to 100 Hz. It is unlikely that there will be an impact on synchronizer engagement (De la Cruz et al., 2010). The generalized equation of motion is:

$$I\ddot{\theta} - C\dot{\theta} - K\theta = T \tag{1}$$

Where I is the inertia matrix in kg-m^2, C is the damping matrix in Nm-s/rad, K is the stiffness matrix in Nm/rad, T is the torque vector in Nm, and θ is the rotational displacement in rad, $\dot{\theta}$ is the angular velocity in rad/s and $\ddot{\theta}$ is the angular acceleration in rad/s^2. Gear ratios are represented as γ for the transmission reduction pairs, and final drive pairs. Equations of motion for each element are:

$$I_e\ddot{\theta}_e - K_e(\theta_\mathrm{F} - \theta_e) = T_e \tag{2}$$

$$I_\mathrm{F}\ddot{\theta}_F + K_e(\theta_\mathrm{F} - \theta_e) - K_\mathrm{F}(\theta_{\mathrm{C}1} - \theta_F) - C_F(\dot{\theta}_{\mathrm{C}1} - \dot{\theta}_\mathrm{F}) = 0 \tag{3}$$

$$\begin{aligned} I_{\mathrm{C}1}\ddot{\theta}_{C1} + K_\mathrm{F}(\theta_{\mathrm{C}1} - \theta_F) + C_F(\dot{\theta}_{\mathrm{C}1} - \dot{\theta}_\mathrm{F}) - C_C(\dot{\theta}_{\mathrm{C}2} - \dot{\theta}_{\mathrm{C}1}) \\ = -(T_\mathrm{C}) \end{aligned} \tag{4}$$

$$\begin{aligned} I_{\mathrm{C}2}\ddot{\theta}_{C2} + C_\mathrm{C}(\dot{\theta}_{\mathrm{C}2} - \dot{\theta}_{C1}) - K_{is}(\theta_{\mathrm{g}1} - \theta_{c2}) - C_{is}(\dot{\theta}_{\mathrm{g}1} - \dot{\theta}_{c2}) \\ = T_\mathrm{C} \end{aligned} \tag{5}$$

$$\begin{aligned} \ddot{\theta}_{g1}(\gamma_1^2 I_{\mathrm{g}2} + I_{\mathrm{g}1}) + K_{is}(\theta_{\mathrm{g}1} - \theta_{c2}) + C_{\mathrm{is}}(\dot{\theta}_{\mathrm{g}1} - \dot{\theta}_{C2}) \\ - \gamma_1 K_{os}(\theta_{d1} - \gamma_1\theta_{\mathrm{g}1}) \\ - \gamma_1 C_{os}(\dot{\theta}_{d1} - \gamma_1\dot{\theta}_{\mathrm{g}1}) = 0 \end{aligned} \tag{6}$$

$$\begin{aligned} \ddot{\theta}_{d1}(\gamma_2^2 I_{\mathrm{d}2} + I_{\mathrm{d}1}) + K_{os}(\theta_{\mathrm{d}1} - \gamma_1\theta_{\mathrm{g}1}) + C_{\mathrm{os}}(\dot{\theta}_{\mathrm{d}1} - \gamma_1\dot{\theta}_{g1}) \\ - \gamma_2 K_d(\theta_W - \gamma_2\theta_{\mathrm{d}1}) \\ - \gamma_, C_d(\dot{\theta}_W - \gamma_,\dot{\theta}_{\mathrm{d}1}) = 0 \end{aligned} \tag{7}$$

$$\begin{aligned} \ddot{\theta}_{d1}(\gamma_2^2 I_{\mathrm{d}2} + I_{\mathrm{d}1}) + K_{os}(\theta_{\mathrm{d}1} - \gamma_1\theta_{\mathrm{g}1}) + C_{\mathrm{os}}(\dot{\theta}_{\mathrm{d}1} - \gamma_1\dot{\theta}_{g1}) \\ + K_m(\theta_{\mathrm{d}1} - \theta_\mathrm{m}) \\ + C_m(\dot{\theta}_{\mathrm{d}1} - \dot{\theta}_\mathrm{m}) - \gamma_2 K_d(\theta_W - \gamma_2\theta_{\mathrm{d}1}) \\ - \gamma_, C_d(\dot{\theta}_W - \gamma_,\dot{\theta}_{\mathrm{d}1}) = 0 \end{aligned} \tag{8}$$

$$I_\mathrm{W}\ddot{\theta}_W + K_d(\theta_\mathrm{W} - \gamma_,\theta_{d1}) + C_\mathrm{d}(\dot{\theta}_\mathrm{W} - \gamma_,\dot{\theta}_{\mathrm{d}1}) = T_\mathrm{W} \tag{9}$$

$$I_\mathrm{m}\ddot{\theta}_m + K_m(\theta_\mathrm{m} - \theta_{d1}) - C_\mathrm{d}(\dot{\theta}_{\mathrm{d}1} - \dot{\theta}_\mathrm{m}) = -T_\mathrm{m} \tag{10}$$

If the clutch is engaged, equations (4) and (5) are unified and the inertias of the clutch members combine. Equation (11) is the eventuating equation of motion. With the clutch engaged, the total number of degrees of freedom of the system decreases. If the clutch is disengaged, then the system has eight degrees of freedoms, while if the clutch is engaged, there are only 7 degrees of freedom.

$$\begin{aligned} (I_{\mathrm{C}2} + I_{\mathrm{C}1})\ddot{\theta}_C + K_\mathrm{F}(\theta_\mathrm{C} - \theta_F) + C_F(\dot{\theta}_\mathrm{C} - \dot{\theta}_\mathrm{F}) \\ - K_{is}(\theta_{\mathrm{g}1} - \theta_\mathrm{c}) - C_{is}(\dot{\theta}_{\mathrm{g}1} - \dot{\theta}_\mathrm{c}) = 0 \end{aligned} \tag{11}$$

When looking at a mild hybrid powertrain, equation (10) is introduced along with equation (8),

which is used instead of equation (7), which is used when analyzing a conventional powertrain.

2.3 *Free vibration analysis*

Vehicle modes, damping ratios, and natural frequencies are used in determining damped free vibration analysis. This requires the representation of the model in state-space form. The externally applied torques are assigned a zero value for free vibration. The equations are then presented in matrix form, as:

$$[I]\{\dot{\theta}\} + [C]\{\dot{\theta}\} + [K]\{\theta\} = \{0\} \quad (12)$$

Damped free vibration analysis is performed using the system matrix taken from equation (12). The application of the eigenvalue problem can be used to determine natural frequencies and damping ratio. The system matrix is as represented as:

$$A = \begin{bmatrix} 0 & \bar{I} \\ I^{-1}C & I^{-1}K \end{bmatrix} \quad (13)$$

where **A** is the system matrix, and $\bar{\mathbf{I}}$ is the identity matrix. The natural frequencies and damping ratios are tabulated in Table 1. With the clutch open there are two rigid body modes as the two separate power train halves are effectively not coupled. In addition to this, each of the open natural frequencies is associated with the two separate bodies; the higher frequency for the engine and clutch disc with low stiffness and high inertia, and the lower frequency for the transmission and vehicle body. However, with the clutch closed the damping ratios are fundamentally identical and the natural frequencies are reasonably close. This remains constant with the change in effective inertia experienced by the locked drum and transmission inertias coupled via reduction gear pairs. The damped free vibration of the powertrain is accomplished using state-space methods. Matrices for *I, C, K* are developed and merged into the system matrix and the eigenvalue problem is solved for the damped natural frequencies of the system. The un-damped natural frequency and damping ratio are identified using real and imaginary components.

Free vibration analysis is used in this paper to compare powertrain models with and without a motor. Damped free vibration analysis is applied to both models, with a presentation of natural frequencies and damping ratios for both models. The relationships of natural frequencies to the model are identified using modal shapes. Important characteristics of the powertrain are derived from the damped free vibration results. Damping ratio results demonstrate the lightly damped nature of the powertrain, where no damping ratio exceeds 10% (as represented in Table 2). Light damping provides more sources of excitation in the powertrain resulting from non-linearities, which can contribute to the initiation of high-frequency vibration in the propeller shaft. This eventuates in one rigid body mode of the powertrain and seven natural frequencies with corresponding damping ratios. Solutions to the eigenvalue problem resulted in 7 paired solutions with real and imaginary components. For each of these proposed solutions, the real component of the eigenvalue was negative, which indicates a mathematically stable system. For the purposes of clarity, zeros are omitted from matrices. The natural frequency of the Rigid Body Mode (RBM) included a small imaginary component as a result of the use of grounded damping elements, however this does not have a bearing on the stability of the system. For the open clutch model, two RBM are present, whereas for each of the closed clutch models one RBM is present.

Compared with the original drivetrain, the design system has one more degree of freedom so there is one more state of natural frequency; the high-frequency response is higher than the original drivetrain, yet for lower frequency response, there is negligible difference. Based on this, it can be concluded that inserting an electric motor with additional inertia does not have a significant effect on low-frequency response.

2.4 *Single dry clutch model*

The preferred model describes the system in a piece-wise manner, with one equation describing the slipping phase and another describing the sticking phase of the clutch. Equation (14) represents the torque through the clutch while slipping. The sticking of the clutch is sustained as long as the torque transmitted through clutch (T_c) remains below the maximally transmittable torque T_c^{max} , which is given by equation (15) (Serrarens et al., 2004, Heijden et al., 2007, BĂȚĂUȘ et al., 2011),

$$T_c = -F_n \mu R_a sign(\omega_e - \omega_c) \quad (14)$$

$$T_c^{max} = F_n \mu_{stick} R_a sign(T_c) \quad (15)$$

$$R_a = \frac{2}{3}\left(\frac{r_o^3 - r_i^3}{r_o^2 - r_i^2}\right) \quad (16)$$

where μ is the dynamic friction coefficient, the rotational speed of the clutch disc and transmission input shaft are presented by ω_e, ω_c , respectively; R_a is active radius of the clutch plates, and F_n is the pressure load on the clutch. $\mu_{stick} = 2.\mu$. Furthermore, the term sign(T_c) is non-positive in the case of vehicle (engine) braking and positive in all other cases; r_o is external diameter of clutch friction plate and r_i is inner diameter of clutch friction plate.

2.5 *Vehicle torque model*

The vehicle resistance torque is distinguished from a combination of road grade, rolling resistance of the vehicle, and aerodynamic drag interactions with weight and gradeability factors as follows:

$$T_v = (\mu M_v g \cos \emptyset + M_v g \sin \emptyset + \frac{1}{2} C_D \rho A_v V_v^2) r_w \quad (17)$$

where T_v is vehicle torque, V_v, m, A_v are the speed, mass and frontal area of the vehicle respectively; r_w is the wheel radius, μ is the rolling resistance (friction) coefficient, C_D and ρ are the drag coefficient and air density respectively, $\emptyset$ is the road grade and g is gravitational acceleration (Borhan et al., 2009, Hartani et al., 2010).

2.6 *Motor and Engine model*

The Simscape environment was used to establish the physical simulation models of the engine and its control. As the engine model only plays a role in providing torque output and speed for a given throttle command, the simple engine model "Generic Engine" in the SimDriveline package is chosen directly, as used in (Zhou et al., 2015, Mahapatra et al., 2008). The physical simulation models of the EPS (motor and control) were also established in the MathWorks' Simscape environment. Look-up tables were used to directly find the output torque based on a set of directed throttle commands and motor speed. The look-up table utilized in the model presented is acquired from ADVISOR on the basis of the Unique Mobility 10 kW Brushless motor. Figure 4 shows the SIMULINK implementation of motor (Johri and Filipi, 2010, Lin et al., 2003).

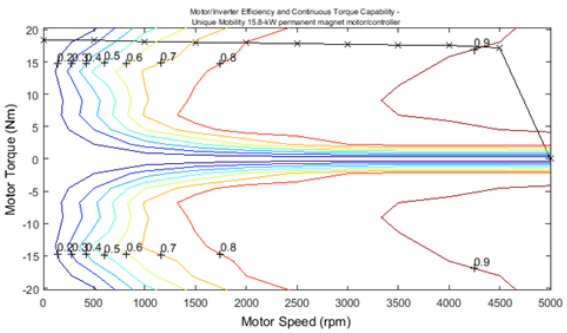

Figure 4. Brushless motor Model in SIMULINK.

3 SIMULATION

The Simscape simulation was performed using the ODE23t element from the ODE suite with a maximum time step of 10^{-1} for the powertrain model, and relative tolerance set to 10^{-3}. State flow event functions were used to ascertain lockup conditions and move between powertrain models. The primary focus of results are on the electric drive mode part and an evaluation of the transient response of both drivetrains. For initial data comparison with between models, a single cycle of the Rural Driving cycle (RDC) was used. Its simplicity and utilization of five up-shifts over its duration was the basis of its selection. The speed of the input shaft (i.e. engine speed) differs according to the different gear ratios of initial and target gear and the throttle angle during the gear change. Results show the difference in magnitude of the torque hole between the conventional and torque-fill powertrains. There is a focus on the variation in shaft speed due to different gear ratios and comparison on the transient response. Figure 5 shows the velocity of the vehicle during an acceleration event 0-100km/h. A fixed throttle angle profile results in a reduced acceleration time by approximately 1.5 seconds using the torque-fill drivetrain, with a marked reduction in deceleration at each gear shift.

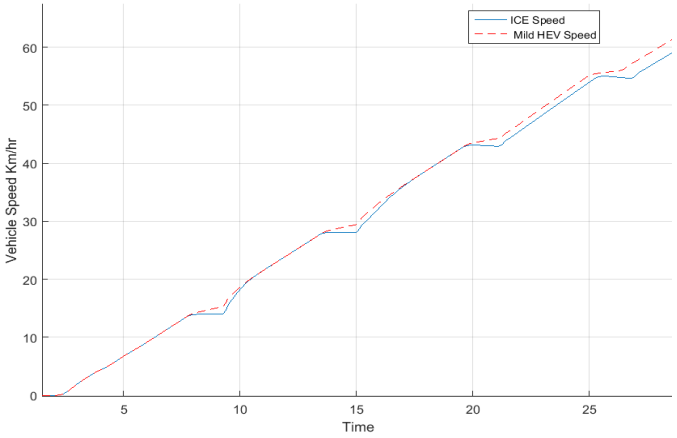

Figure 5. Speed profile in ICE and Mild HEV models

A representation of the output shaft torque of the conventional and mild HEV drivetrain when upshifting sequentially from 2nd to 5th gear is seen in Figure 6. Three discrete torque oscillation responses are in each upshift event. The first torque excitation is caused by disengaging the clutch. When the clutch is decoupled, the engine and flywheel inertia are decoupled from the transmission. This sudden change in inertia results in excitation of torque response. Synchronizing gears causes a second, smaller excitation. As the previous gear is desynchronized and the next gear is locked to the output shaft, there is a variation in layshaft speed due to the energy absorbed by the synchronizer along with windage and bearing losses. When the clutch is re-engaged, the third spike occurs. A torque overshoot can occur due to different rotational speeds between the flywheel and clutch disc (Fredriksson and Egardt, 2000). The torque excitations on the output shaft are clearly illustrated in Figure 6. The torque profiles of the original drivetrain and the torque-fill drivetrain are contrasted. When the system is operating in torque fill-in mode, it is apparent that the torque hole is re-

duced, along with a marked reduction in the oscillatory peak by approximately 175 Nm.

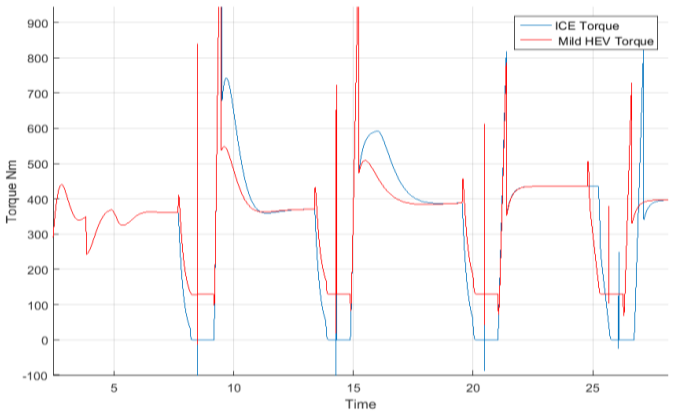

Figure 6. Torque profile.

4 CONCLUSION

This paper has introduced a mild hybrid powertrain for a manual transmission vehicle, integrating an electric machine to provide drivability and comfort by reducing torque holes during gear shifts. The adoption of the motor has required the development of vehicle control strategies for shifting to compensate for lower powertrain system damping than what is present in a conventional powertrain and the resulting transient vibration during and after gearshift. This paper has presented a strategy for up-shifting that employs the increased electric motor functionality to decrease the torque hole. The torque-fill drivetrain can be used equally successfully with automated manual, and traditional manual gearboxes, and the limited motor power and duty cycle limit the size and cost of other system components, such as batteries and converters. Due to the intermittent operation, it is also possible to safely operate the components beyond their rated continuous output and yield greater benefit.

Definitions/Abbreviations

ICE	Internal Combustion Engine
MHEV	Mild Hybrid Electric Vehicles
MT	Manual Transmission
EPS	electric propulsion system
RBM	The rigid body mode

Model parameters

Name	Symbol	Units
Torque	T	Nm
Equivalent Inertia	I	Kg m2
Speed	ω	rad/s
Displacement	Θ	rad
Torsional stiffness	K	Nm/rad
Friction Coefficient	C	Nms/rad

Component	Symbol
Engine	e
Flywheel	F
Clutch drum	$C1$
Clutch hub	$C2$
Input Shaft	is
Gearbox	g
Output shaft	os
Differential	d
Motor	m
Vehicle with tyre	W

Appendix

1. Parameters

Parameter	Damping (Nm/rad)	Parameter	Stiffness (Nm/rad)
C_F	2	K_e	95000
C_{c}	0.049	K_F	2000
C_{is}	0.0044	K_{is}	5600
C_{os}	0.1	K_{os}	4700
C_{d}	0.1	K_{m}	9500
C_{m}	0.0045	K_{d}	65000

Parameter	Inertia (kg-m2)
I_e	0.4
I_F	0.2
I_{c1}	0.0072
I_{c2}	0.0125
I_{g1}	0.0006
I_{g2}	0.0013
I_{d1}	0.16
I_{d2}	1.6
I_m	0.0045
I_w	167.558

2. Results

Table 1. Damped free vibration results of ICE powertrain and mild HEV with 1st gear.

ICE Model		
Frequency number	Natural frequency $\boldsymbol{\omega}_n$(Hz)	Damping ratio ζ (%)
1	312.6261	1.901
2	134.9499	0.62
3	96.3400	8.41
4	10.1634	0.07
5	7.7347	1.71
6	0	-

Mild HEV Model		
Frequency number	Natural frequency $\boldsymbol{\omega}_n$ (Hz)	Damping ratio ζ (%)
1	312.6261	1.901
2	231.2795	0.03
3	134.9499	0.62
4	96.3400	8.41
5	10.1620	0.07
6	7.7347	1.71
7	0	-

Table 2. Natural frequencies of each gear ratio.

	Original Drivetrain				
Mode	1st	2nd	3rd	4th	5th
1	312.6261	328.1553	347.1295	369.5351	390.5757
2	134.9499	134.9582	134.9641	134.9683	134.9707
3	96.3400	90.8719	84.7693	78.2564	72.7143
4	10.1634	10.1972	10.2374	10.2829	10.3238
5	7.7347	7.5326	7.2535	6.8690	6.4384
6	0	0	0	0	0

	Mild HEV				
Mode	1st	2nd	3rd	4th	5th
1	312.6261	328.1553	347.1295	369.5351	390.5757
2	231.2795	231.2795	231.2795	231.2795	134.9707
3	134.9499	134.9582	134.9641	134.9683	231.2795
4	96.3400	90.8719	84.7693	78.2564	72.7143
5	10.1620	10.1958	10.2360	10.2815	10.3224
6	7.7347	7.5326	7.2535	6.8690	6.4384
7	0	0	0	0	0

3. Specifications

Table 3. Vehicle Global Specifications.

Component	Parameter	SI Units
Vehicle	Mass with hybrid	1600 kg
	Frontal area	3 m^2
	Drag coefficient	0.4
	Distance from CG to front axle	1.7 m
	Distance from CG to rear axle	2 m
	CG height	0.5 m
	Tire rolling radius	0.312 m
Engine	Maximum power	70 kW
	Speed at maximum power	5500 RPM
	Maximum speed	7000 RPM
	Cylinders	4
Motor	Voltage	96 V
	Maximum power output	10 kW
	Maximum torque	54 Nm

REFERENCES

AOKI, K., KURODA, S., KAJIWARA, S., SATO, H. & YAMAMOTO, Y. 2000. Development of integrated motor assist hybrid system: development of the'insight', a personal hybrid coupe. Honda R and D Co., Ltd.(US).

BARASZU, R. & CIKANEK, S. Torque fill-in for an automated shift manual transmission in a parallel hybrid electric vehicle. American Control Conference, 2002. Proceedings of the 2002, 2002. IEEE, 1431-1436.

BARASZU, R. C. & CIKANEK, S. R. 2003. Hybrid electric vehicle with motor torque fill in. *Ford Motor Company*. Google Patents.

BĂȚĂUȘ, M., MACIAC, A., OPREAN, M. & VASILIU, N. 2011. Automotive Clutch Models for Real Time Simulation. *Proceedings of the Romanian Academy, Series A: Mathematics, Physics, Technical Sciences, Information Science*.

BORHAN, H. A., VAHIDI, A., PHILLIPS, A. M., KUANG, M. L. & KOLMANOVSKY, I. V. Predictive energy management of a power-split hybrid electric vehicle. American Control Conference, 2009. ACC'09., 2009. IEEE, 3970-3976.

CHANG, L. 1994. Comparison of AC drives for electric vehicles-a report on experts' opinion survey. *Aerospace and Electronic Systems Magazine, IEEE,* 9**,** 7-11.

CROWTHER, A. & ZHANG, N. 2005. Torsional finite elements and nonlinear numerical modelling in vehicle powertrain dynamics. *Journal of Sound and Vibration,* 284**,** 825-849.

CROWTHER, A. R., SINGH, R., ZHANG, N. & CHAPMAN, C. 2007. Impulsive response of an automatic transmission system with multiple clearances: Formulation, simulation and experiment. *Journal of Sound and Vibration,* 306**,** 444-466.

DE LA CRUZ, M., THEODOSSIADES, S. & RAHNEJAT, H. 2010. An investigation of manual transmission drive rattle. *Proceedings of the Institution of Mechanical Engineers, Part K: Journal of Multi-body Dynamics,* 224**,** 167-181.

FREDRIKSSON, J. & EGARDT, B. Nonlinear control applied to gearshifting in automated manual transmissions. Decision and Control, 2000. Proceedings of the 39th IEEE Conference on, 2000. IEEE, 444-449.

GALVAGNO, E., VELARDOCCHIA, M. & VIGLIANI, A. 2009. A model for a flywheel automatic assisted manual transmission. *Mechanism and Machine Theory,* 44**,** 1294-1305.

HARTANI, K., MILOUD, Y. & MILOUDI, A. 2010. Improved direct torque control of permanent magnet synchronous electrical vehicle motor with proportional-integral resistance estimator. *Journal of Electrical Engineering and Technology,* 5**,** 451-461.

HEIJDEN, A. V. D., SERRARENS, A., CAMLIBEL, M. & NIJMEIJER, H. 2007. Hybrid optimal control of dry clutch engagement. *International Journal of Control,* 80**,** 1717-1728.

JOHRI, R. & FILIPI, Z. 2010. Low-cost pathway to ultra efficient city car: Series hydraulic hybrid system with optimized supervisory control.

KUO, K.-L. 2011. Simulation and Analysis of the Shift Process for an Automatic Transmission. *World Academy of Science, Engineering and Technology,* 52**,** 341-347.

LIN, C.-C., PENG, H., GRIZZLE, J. W. & KANG, J.-M. 2003. Power management strategy for a parallel hybrid electric truck. *Control Systems Technology, IEEE Transactions on,* 11**,** 839-849.

MAHAPATRA, S., EGEL, T., HASSAN, R., SHENOY, R. & CARONE, M. 2008. Model-based design for hybrid electric vehicle systems. SAE Technical Paper.

RAHMAN, Z., BUTLER, K. L. & EHSANI, M. 2000. A comparison study between two parallel hybrid control concepts. *Development,* 1**,** 0978.

RAO, S. S. 2011. *Mechanical Vibrations*, Upper Saddle River, N.J. : Prentice Hall.

SERRARENS, A., DASSEN, M. & STEINBUCH, M. Simulation and control of an automotive dry clutch. American Control Conference, 2004. Proceedings of the 2004, 2004. IEEE, 4078-4083.

SHARMA, S. & KUMAR, V. 2013. Optimized Motor Selection for Various Hybrid and Electric Vehicles. SAE Technical Paper.

SUN, Z. & HEBBALE, K. Challenges and opportunities in automotive transmission control. American Control Conference, 2005. Proceedings of the 2005, 2005. IEEE, 3284-3289.

WAGNER, G. 2001. Application of transmission systems for different driveline configurations in passenger cars. SAE Technical Paper.

WAGNER, U. & WAGNER, A. 2005. Electrical shift gearbox (esg)-consistent development of the dual clutch transmission to a mild hybrid system. SAE Technical Paper.

ZERAOULIA, M., BENBOUZID, M. E. H. & DIALLO, D. 2006. Electric motor drive selection issues for HEV propulsion systems: A comparative study. *Vehicular Technology, IEEE Transactions on,* 55**,** 1756-1764.

ZHOU, Z., ZHANG, J., XU, L. & GUO, Z. Modeling and simulation of hydro-mechanical continuously variable transmission system based on Simscape. Advanced Mechatronic Systems (ICAMechS), 2015 International Conference on, 2015. IEEE, 397-401.